

# Millimeterwave Radar High-Resolution Imaging via OFDM Waveforms

Wen-Qin Wang, *Member, IEEE*

1. Sch. of Comm. & Info. Eng., UESTC, Chengdu  
2. Henan Key Lab. of Coal Mine Methane and Fire  
Prevention, Henan University, Henan, P. R. China  
e-mail: wqwang@uestc.edu.cn

Jingye Cai, *Member, IEEE*

School of Communication and Information Engineering  
University of Electronic Science and Technology of  
China (UESTC), Chengdu, P. R. China  
e-mail: jycai@uestc.edu.cn

**Abstract**—A novel combination of millimeterwave linearly frequency modulated (LFM) technology and new radar imaging techniques can provide a good high-resolution imaging sensor that can be inboard in unmanned vehicles, in which stringent limitations of size, weight and power consumption are required. This paper presents an approach of multiple transmission and multiple reception in elevation for vehicle-borne millimeterwave radar high-resolution imaging. This radar employs orthogonal frequency diversity modulated (OFDM)-LFM waveforms, so as to obtain a high-resolution imagery over a wide swath coverage. The system concepts, geometry relations and signal models are provided. Computer simulation examples are also performed. Additionally, the generation of the OFDM waveforms with parallel direct digital synthesizer (DDS)-driven phase locked loop (PLL) synthesizer is discussed, and the block diagram of the synthesizer is provided.

**Keywords**—Waveform diversity; orthogonal frequency diversity modulation (OFDM); radar imaging; millimeterwave radar; waveform generator.

## I. INTRODUCTION

Unmanned vehicle-borne radars have received much recognition in recent years; however, to integrate a high-resolution imaging radar into unmanned vehicles, stringent limitations of size, weight, and power consumption should be satisfied. Millimeterwave linearly frequency modulated (LFM) radar requires only a much lower transmit power [1, 2]. Thus, a combination of millimeterwave LFM technology and SAR processing techniques can provide an optimal solution. For these reasons, millimeterwave imaging radar, especially synthetic aperture radar (SAR) has become a research hot in recent years. SAR imagery is derived through correlating the raw data with a two-dimensional reference function. The range resolution is obtained by transmitting wideband signals, and the azimuth resolution is obtained by exploiting the relative motion between the radar platform and the imaged targets. However, there is a possible in range ambiguity and/or azimuth ambiguity. Range ambiguity can be reduced by employing a waveform with adequate duration to detect the farthest echo, but the corresponding azimuth ambiguity will be introduced. Alternatively, azimuth ambiguity can be reduced by reducing waveform repetition period but, consequently, creates range ambiguity.

In this paper, we describe an approach of multiple transmission and multiple reception in elevation for unmanned vehicle-borne millimeterwave radars. By applying

orthogonal frequency modulated (OFDM)-LFM waveform, range ambiguity or azimuth ambiguity can be reduced, so that the high-resolution and wide-swath remote sensing is possible. The system configuration and signal models or relations are detailed. The waveform properties are analyzed and simulated. To generate the required OFDM-LFM waveform, one parallel direct digital synthesizer (DDS)-driven phase locked loop (PLL) synthesizer is described.

The remaining sections are organized as follows. Section II develops the new system configuration of vehicle-borne millimeterwave SAR with multiple transmissions in elevation. Next, example OFDM-LFM waveform is designed and its properties are analyzed in Section III, followed by the parallel DDS-driven PLL synthesizer used for synthesizing the required OFDM-LFM waveforms in Section IV. Finally, Section V concludes the paper.

## II. SYSTEM GEOMETRY AND SIGNAL MODELS

Referring to SAR imaging, it is a contradiction to simultaneously obtain both unambiguous high resolution and wide swath. The ground swath  $W_s$  is determined by the antenna width  $w_a$  with  $\lambda$  the radar wavelength. If  $R_c$  is the slant range from radar to mid-swath, then there is [3]

$$W_s \approx \frac{\lambda R_c}{w_a \cos(\eta)} \quad (1)$$

where  $\eta$  is the incidence angle. A basic limitation is the minimum antenna area constraint, which can be represented by

$$A_a = w_a w_l \geq \frac{4v_a \lambda R_c \tan(\eta)}{c_o} \quad (2)$$

where  $w_l$  is the antenna length,  $v_a$  is the platform velocity, and  $c_o$  is the speed of light. This requirement arises because the illuminated ground area must be restricted so that the radar does not receive ambiguous echoes in range and/or azimuth (Doppler). In this respect, a high operating pulse repeated frequency (PRF) is desirable to suppress azimuth ambiguity. But the magnitude of the operating PRF is limited by range ambiguity.

The attainment of wide-swath will become increasingly difficult if higher azimuth resolution is required, due to the requirement of increased PRF. To overcome this limitation, several innovative techniques using multiple receive

apertures have been suggested [4-6]. However, only one waveform is employed in these methods. This paper further overcomes the minimum antenna area constraint by using multiple transmission and multiple reception in elevation.

Figure 1 shows the basic scheme of orthogonal multiple transmission and multiple reception in elevation. That is, orthogonal waveforms are transmitted from different subantennas of the transmitter to illuminate a wide swath. Each subantenna of the receiver can receive all the transmitted signals. If  $M$  transmit subantennas and  $N$  ( $M = N$  is assumed in this paper) receive subantennas are employed,  $M \times N$  different returns can be observed by the receiver. For the  $i$ th transmit subantenna and  $j$ th receive subantenna, the radar response function can be approximated as a realization of random process denoted by  $a_{j,i}$ .

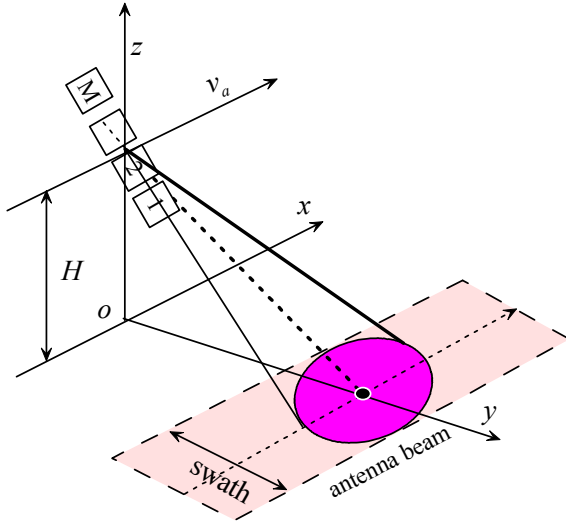


Figure 1. Geometry of MIMO configuration in elevation.

The received signal at the  $j$ th receive subantenna due to the  $i$ th transmit waveform can be represented by

$$r_{j,i}(t) = s_i(t, j) a_{j,i} + n_j(t) \quad (3)$$

The term  $n_j(t)$  is an additive noise process independent of the response function  $a_{j,i}$ . The term  $s_i(t, j)$  denotes the  $i$ th transmitted signal modified according to the radar channel characteristics for the  $j$ th receive subantenna. The received signal will most likely be sampled; thus, it can be represented by

$$\mathbf{r}_{j,i} = \mathbf{s}_i(j) a_{j,i} + \mathbf{n}_j \quad (4)$$

As there are  $M$  transmit waveforms, the received signals at the  $j$ th receive subantenna is the linear combination of all such signals as

$$\mathbf{r}_j = \sum_{i=1}^M \mathbf{r}_{j,i} = \sum_{i=1}^M \mathbf{s}_i(j) a_{j,i} + \mathbf{n}_j = \mathbf{s}_j \mathbf{a}_j + \mathbf{n}_j \quad (5)$$

The term  $\mathbf{s}_j$  is a matrix whose columns are the vectors  $\mathbf{s}_i(t)$ . As there are total of  $N$  receive subantennas, the data from each can be combined into a single vector

$$\mathbf{r}_j = \begin{bmatrix} s(1) & 0 & \cdots & 0 \\ 0 & s(2) & \cdots & 0 \\ \vdots & \vdots & \ddots & \vdots \\ 0 & 0 & 0 & s(N) \end{bmatrix} \cdot \begin{bmatrix} \mathbf{a}_1 \\ \mathbf{a}_2 \\ \vdots \\ \mathbf{a}_N \end{bmatrix} + \begin{bmatrix} \mathbf{n}_1 \\ \mathbf{n}_2 \\ \vdots \\ \mathbf{n}_N \end{bmatrix} \quad (6)$$

$$= \mathbf{s} \cdot \mathbf{a} + \mathbf{n}$$

where  $\mathbf{s} = \text{diag}[s(1), s(2), \dots, s(N)]$  with  $\text{diag}$  a diagonal operator and  $\mathbf{a} = [a(1), a(2), \dots, a(N)]^T$ . The term  $^T$  denotes a transpose. This equation is just the signal model used for describing the received radar data due to a set of transmit waveforms with the response vector  $\mathbf{a}$ .

Finally, each of the received data is mixed, digitized and stored. A posteriori, digital beamforming on receive can then be carried out by a joint spatiotemporal processing of the collected subantenna signals. Equivalently, a large beam can then be obtained.

### III. OFDM WAVEFORM

Each transmit subantenna should transmit a unique waveform, orthogonal to the waveforms transmitted by the other subantennas. This requirement is similar to MIMO radar which has received much attention [7-9]. One polyphase code for orthogonal netted radars was presented in [10], but the Doppler effect was not considered. Moreover, an additional requirement is that the transmitted waveform should have a big product of time-width and frequency-width and a constant amplitude, so as to achieve a high range resolution and reduce the required peak transmit power. We have investigated the up-chirp and down-chirp waveforms in [11]. But, we extend it into random OFDM-LFM waveform, as shown in Fig. 2.

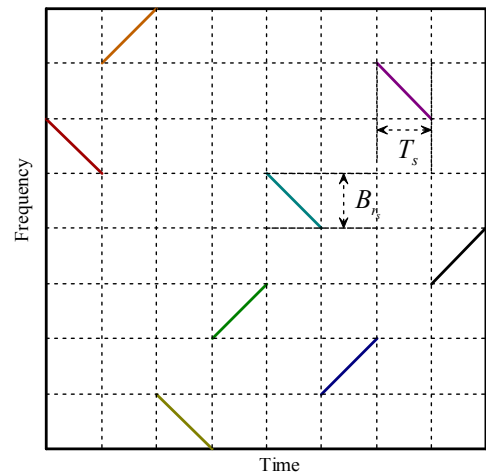


Figure 2. One example MIMO-OFDM waveform.

The transmitted random OFDM-LFM waveform can be expressed as

$$s(t) = \sum_{m=1}^M s_m(t) = \sum_{m=1}^M \exp \left[ j2\pi \left( f_m t + \frac{1}{2} k t^2 \right) \right], 0 < t < T_s \quad (7)$$

where  $f_m$  is the randomly selected subpulse frequency center between  $f_c - B_r/2 < f_i < f_c + B_r/2$  with each subpulse having a bandwidth of  $B_{r_s} = B_r/N$ , where  $f_c$  is the equivalent radar frequency center,  $B_r$  is the radar bandwidth,  $T_s$  is the subpulse duration, and  $M$  is just the number of subpulses. It has been investigated that the LFM waveforms with inverse chirp rate have a good orthogonality [11]. It is shown that, if the LFM waveforms with the same chirp rate and  $|f_m - f_n| = B_{r_s}$  or  $|f_m - f_n| = 2B_{r_s}$  are used, the corresponding radar returns can be separated during subsequent data processing. It is also deduced that using the LFM waveforms with the same chirp rate and  $|f_m - f_n| \geq 3B_{r_s}$  offers an additional suppression of the cross-correlation components. However, this also means a wider total transmit/receive bandwidth for the RF hardware of the radar system.

Next, each receive subantenna's signals are mixed, digitized and stored. Multi-beam forming in elevation can then be carried out. For each of the transmitted  $M$  waveforms, there are  $N$  coherent returns. After matched filtering, the range resolution for each subantenna channel can be represented by

$$|z_{out}(t)| = \left| \frac{\sin[\pi B_{r_s}(t-\tau)]}{\pi B_{r_s}(t-\tau)} \cdot \frac{\sin[M\pi B_{r_s}(t-\tau)]}{\sin[\pi B_{r_s}(t-\tau)]} \right| \quad (8)$$

Note that the amplitude terms are ignored. The equivalent range resolution is  $\rho_r = c_o/2MB_{r_s}$ . As shown Fig. 3, if  $M$  orthogonal LFM waveforms are employed, after spectrum synthesis the equivalent range resolution can be improved by  $M$  times of the radar using a frequency bandwidth of  $B_{r_s}$ . In this way, high range resolution can be obtained. More importantly, if the matched filter outputs are fed to multiple digital filters with their coefficients designed for different beam-pointing directions, multiple pairs of virtual transmitting and receiving beams can be formed simultaneously with the same gain without increasing transmitting power. This scheme is shown in Fig. 4.

#### IV. WAVEFORM SYNTHESIS WITH PARALLEL DDS

Existing waveform synthesizer can be classified into DDS, PLL synthesizer, and DDS-driven PLL synthesizer. DDS generates high-linearity and agile-frequency, but the transmitted RF LFM signals cannot be directly synthesized because the maximum usable clock frequency of state-of-art commercial DDS devices is limited to 1GHz. PLL synthesizers cannot achieve fast frequency switching speed while an arrow frequency step is required. Moreover, low phase noise and low spur level are also required for the

OFDM-LFM waveforms [12,13]. Otherwise, its imaging performance will degraded greatly [14].

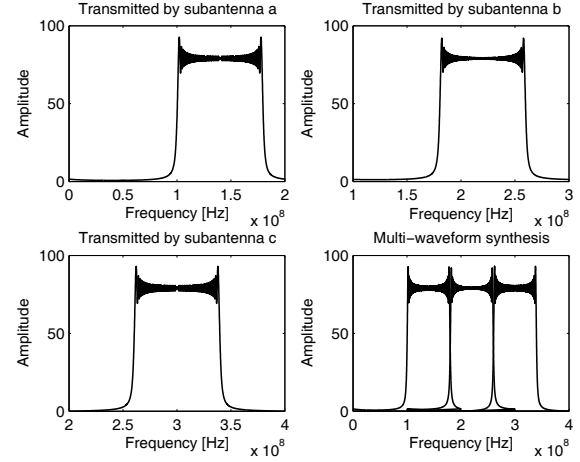


Figure 3. Spectrum synthesis for the received multi-subantenna data.

#### Orthogonal multi-transmission and multi-reception in elevation

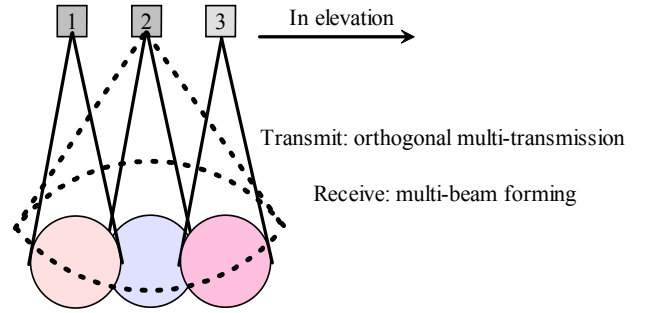


Figure 4. Scheme of multi-beam forming in elevation.

To synthesize high-performance OFDM-LFM waveforms, we propose one parallel configuration of full-coherent PLL synthesizer driven by DDS, as shown in Fig. 5 [16]. Note that only two orthogonal LFM waveforms are shown in this figure. It can be extended into multiple OFDM-LFM waveforms. DDS output frequency is determined by its clock frequency  $f_{clk}$  and an D-bit tuning word  $2^d$  ( $d \in [1, D]$ ) written into its register, where  $D$  is the register length. The value of  $2^d$  is added into an accumulator at each clock update, and the resulting digital wave is converted into an analog wave in the digital-to-analog converter (DAC). The DDS output frequency is determined by

$$f_{DDS} = \frac{f_{clk} \cdot 2^d}{2^D}, d \in [1, 2, 3, \dots, D-1] \quad (9)$$

By continuously increasing the input DDS phase increment, one baseband LFM signal can be synthesized by

$$S_{LFM}(d) = \cos \left[ \pi \frac{BT}{D^2} \left( d - \frac{D}{2} \right)^2 \right] + j \sin \left[ \pi \frac{BT}{D^2} \left( d - \frac{D}{2} \right)^2 \right] \quad (10)$$

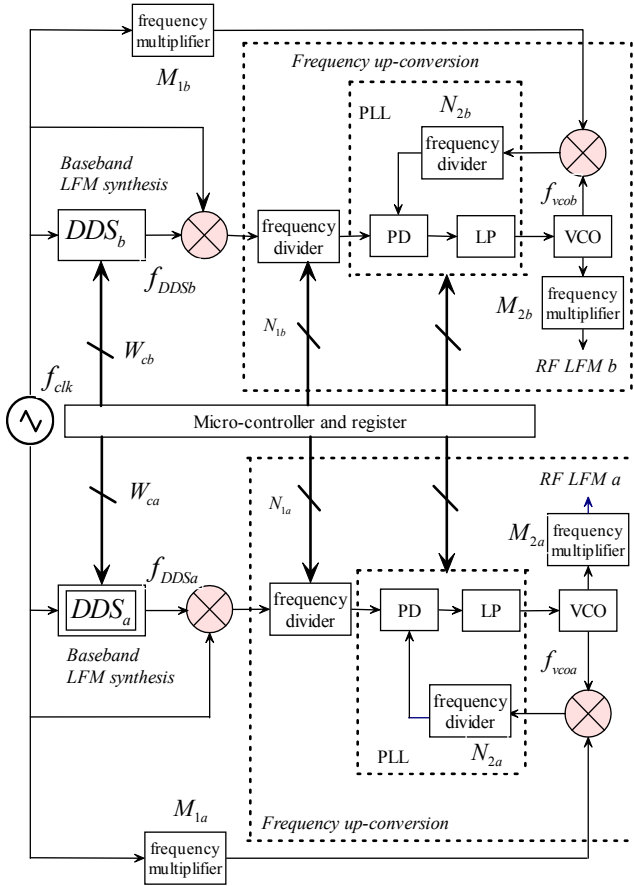


Figure 5. Block diagram of the OFDM-LFM waveform Synthesizer.

Next, the output LFM signals are further up-converted by the wideband frequency multiplier. This waveform generator provides several advantages such as fast frequency switching speed, fine frequency resolution, good spectral purity. More importantly, this approach enables synthesizing OFDM waveforms simultaneously with consistent performance. This may simplify subsequent error compensation and signal processing.

## V. CONCLUSION

This paper presents a scheme of waveform diversity-based millimeterwave radar for high-resolution imaging. Multiple transmission and multiple reception with orthogonal waveforms in elevation is employed. In this way, high range resolution can be obtained with combined matched filtering and multi-spectrum synthesis, and wide-swath or high azimuth resolution can be obtained by multi-

beam forming. Furthermore, a kind of OFDM-LFM waveforms is analyzed, along with one parallel DDS-driven PLL synthesizer which is designed to generate the required diversity waveforms.

## ACKNOWLEDGMENT

This work was supported in part by the Open Fund of the Henan Key Laboratory of Coal Mine Methane and Fire Prevention, Henan University under the contract number of HKLGF200803.

## REFERENCES

- [1] S. Scheiblhofer, S. Schuster, and A. Stelzer, "High-speed FMCW radar frequency synthesizer with DDS based linearization," *IEEE Trans. Microwave Wireless Compon. Lett.*, vol. 19, no. 4, pp. 397–399, May 2007.
- [2] Y. Kimura, A. Senga, M. Sakai, and M. Haneishi, "An alternating-phase fed single-layer slotted waveguide array with a sector shaped beam for millimeter-wave radar applications," *IEICE Trans. Electronics*, vol. E90-C, no. 9, pp. 1801–1806, Sept. 2007.
- [3] A. Currie, and M. A. Brown, "Wide-swath SAR," *IEE Proc.-Radar Sonar Navig.*, vol. 139, no. 2, pp. 122–135, April 1992.
- [4] M. Younis, C. Fischer, and W. Wiesbeck, "Digital beamforming in SAR systems," *IEEE Trans. Geosci. Remote Sens.*, vol. 41, no. 7, pp. 1735–1739, July 2003.
- [5] G. D. Callaghan, and I. D. Longstaff, "Wide-swath spaceborne SAR using a quadelement array," *IEE Proc.-Radar Sonar Navig.*, vol. 146, no. 3, pp. 159–165, June 1999.
- [6] W. Q. Wang, "Near-space wide-swath radar imaging with multiaperture antenna," *IEEE Antennas Wireless Propag. Lett.*, vol. 8, pp. 461–464, Oct. 2009.
- [7] J. Li, and P. Stoica, *MIMO Radar Signal Processing*, Wiley, New York, 2009.
- [8] B. Friedlander, "Waveform design for MIMO radars," *IEEE Trans. Aerosp. Electron. Syst.*, vol. 43, no. 3, pp. 1227–1238, Jul. 2007.
- [9] Y. Yang, and R. S. Blum, "MIMO radar waveform design based on mutual information and minimum mean-square error estimation," *IEEE Trans. Aerosp. Electron. Syst.*, vol. 43, no. 1, pp. 330–343, Jan. 2007.
- [10] H. Deng, and B. Himed, "A virtual antenna beamforming (VAB) approach for radar systems by using orthogonal coding waveforms," *IEEE Trans. Antenna. Propag.*, vol. 57, no. 2, pp. 425–435, Feb. 2009.
- [11] W. Q. Wang, Q. C. Peng, and J. Y. Cai, "Waveform-diversity-based millimeter-wave UAV SAR remote sensing," *IEEE Trans. Geosci. Remote Sens.*, vol. 47, no. 3, pp. 691–700, Mar. 2009.
- [12] W. Q. Wang, J. Y. Cai, and Y. W. Yang, "Extracting phase noise of microwave and millimeter-wave signals by deconvolution," *IEE Proc. Sci. Meas. Tech.*, vol. 153, no. 1, pp. 7–12, Jan. 2006.
- [13] J. M. Zhou, "Spurious reduction techniques for DDS-based synthesizers," *IEICE Trans. Electron.*, vol. E92-C, no. 2, pp. 252–257, Feb. 2009.
- [14] W. Q. Wang, "Analysis of waveform errors in millimeter-wave LFM CW synthetic aperture radar," *Int. J. Infr. Milli. Wave.*, vol. 27, no. 11, pp. 1433–1444, Nov. 2006.
- [15] K. Tajima, Y. Imai, and Y. Kanagawa, "Low spurious frequency setting algorithm for a triple type PLL synthesizer driven by a DDS," *IEICE Trans. Electron.*, vol. E85C, NO. 3, pp. 595–598, Mar. 2002.
- [16] W. Q. Wang, Q. C. Peng, and J. Y. Cai, "Diversified MIMO SAR waveform analysis and generation," *Proc. Int. Synthetic Aperture Radar Conf.*, Xi'an, China, Oct. 2009, pp. 270–273.